

Green Chemistry

Accepted Manuscript



This is an *Accepted Manuscript*, which has been through the Royal Society of Chemistry peer review process and has been accepted for publication.

Accepted Manuscripts are published online shortly after acceptance, before technical editing, formatting and proof reading. Using this free service, authors can make their results available to the community, in citable form, before we publish the edited article. We will replace this *Accepted Manuscript* with the edited and formatted *Advance Article* as soon as it is available.

You can find more information about *Accepted Manuscripts* in the [Information for Authors](#).

Please note that technical editing may introduce minor changes to the text and/or graphics, which may alter content. The journal's standard [Terms & Conditions](#) and the [Ethical guidelines](#) still apply. In no event shall the Royal Society of Chemistry be held responsible for any errors or omissions in this *Accepted Manuscript* or any consequences arising from the use of any information it contains.



www.rsc.org/greenchem

ARTICLE

Supported Gold Nanoparticles as an Efficient and Reusable Heterogeneous Catalyst for Cycloisomerization Reactions

Cite this: DOI: 10.1039/x0xx00000x

Received 00th January 2012,

Accepted 00th January 2012

DOI: 10.1039/x0xx00000x

www.rsc.org/

Felix Schröder^a, Manuel Ojeda^b, Nico Erdmann^c, Jeroen Jacobs^a, Rafael Luque^b, Timothy Noël^c, Luc Van Meervelt^a, Johan Van der Eycken^d and Erik V. Van der Eycken^{*a}

We report the utilization of a novel catalyst for cycloisomerizations. The novel catalyst system contains gold nanoparticles supported on Al-SBA15, which was prepared by the ball-milling process. We developed a greener methodology for synthesizing spiroindolines under heterogeneous conditions, using this novel class of supported gold nanoparticles in combination with microwave irradiation. The catalyst is highly reusable and selective. Cycloisomerization reaction yields ranged from good to excellent leading to the formation of two novel classes of six- and seven-membered heterocycles, which are unprecedented so far. The selectivity of the catalyst towards the desired products is high and the reaction can be performed in ethanol as solvent. A one-pot cascade reaction could be established commencing with the Ugi-reaction to ensure diversity.

Introduction

Gold catalysis was once completely neglected: however, during the last two decades, it became the new Gold Rush, and is currently intensively investigated in research groups around the world.¹⁻⁵ Homogeneous gold catalysis plays a key role in the field of cycloisomerization reactions⁶⁻⁸ and gold(I) catalysts are well known for their selectivity towards π -systems acting as soft Lewis acids activating double and triple bonds for nucleophilic attacks.^{9,10}

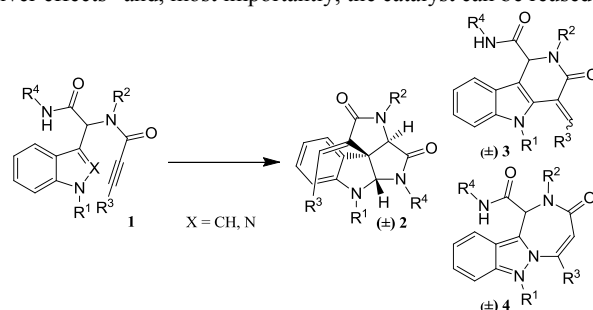
The introduction of a ligand-gold-chloride complex with a silver source is a common procedure in the preparation of homogeneous catalysts. This involves abstracting the chloride anion from the complex and substituting it with a less coordinating counter ion, such as triflate, triflimide or hexafluoroantimonate, to generate the cationic gold species.¹¹ Although this procedure is well established, recent publications show that chloride coordination towards the gold also leads to chloride-bridged digold complexes, which might be less active.^{12,13} In order to exclusively obtain monogold complexes, the use of multiple equivalents of silver salts is reportedly necessary. However, this might result in an unwanted “silver effect.”¹⁴

The use of TiO₂-supported gold nanoparticles (NPs) in cycloisomerization reactions of simple 1,6-enynes¹⁵ and computational studies about the differences and similarities of gold-complexes and gold clusters¹⁶ inspired us to explore utilizing supported gold nanoparticles for the cycloisomerization of complex Ugi-adducts as shown in Scheme 1. This was so far only investigated under homogeneous conditions.^{7,17} Spiroindolines such as perophora-midine¹⁸ and communesin F¹⁹ possess interesting bioactivity and occur naturally. However, convenient synthetic methods are rather limited. Here we present an efficient route to fused heterocycles.

Detailed studies by Corma and colleagues on the catalytically active species of supported gold nanoparticles suggest an active particle diameter within 1–9 nm. Particles this size offer enough

defects such as corners and edges at which the reaction can occur. Furthermore they report the presence of Au(I) and Au(III) species next to Au(0), which is proven by XPS and CO titration.²⁰ In this case the Au(I) species could facilitate alkyne activation. Detailed computational studies investigating the characteristics of Au nanoparticles by Lopez and colleagues¹⁶ as well as Zhang, Tang and colleagues²¹ have been conducted. The former revealed insights into the energies of alkyne/Au NP coordination while the latter provided results on mechanistic studies.

The use of heterogeneous catalysts has multiple advantages: no ligands are required, no silver is introduced which could lead to “silver effects” and, most importantly, the catalyst can be reused.



Scheme 1: Obtained products for post-Ugi-cyclization reactions.

Furthermore, the application of supported gold is well established in multiple chemical processes such as H₂-activation, CO/H₂O-activation and alcohol-activation.²²

For the preparation of metal nanoparticles deposited on various supports a wide variety of methods exist and this toolkit is constantly expanding. Corma and coworkers²³ as well as some authors from this work^{24,25} published critical reviews on chemical and mechanochemical preparation methods. Mechanochemical preparation methods (i.e. ball milling) are gaining importance and

impact due to their simplicity, reproducibility and potential to design advanced nanomaterials for catalytic applications. The increasing interest in this method²⁶⁻³⁰ relies on the excellent characteristics of designed nanomaterials including a narrow nanoparticle size distribution, the possibility of simple scale up and a general reproducibility in the prepared nanocatalysts.

Results and Discussion

The catalyst preparation was performed by first synthesizing Al-SBA15 from tetraethylorthosilicate and aluminium isopropoxide (see SI). Al-SBA15 was then functionalized with gold nanoparticles under mechanochemical ball milling conditions following an established and optimized procedure (see SI). Briefly, the gold precursor (0.083 g $\text{HAuCl}_4 \cdot 3\text{H}_2\text{O}$, equivalent to a theoretical 4 wt% Au in the final material) was milled together with 1 g of Al-SBA-15 in a Retsch PM-100 planetary ball mill under previously optimized milling conditions (350 rpm, 10 min). Upon Au incorporation, the resulting material was calcined at 400 °C (4 h, in air) prior to its use in the reaction. Au@Al-SBA-15 catalysts were characterized using five different techniques including TEM, BET, XRD, XPS and experiments regarding metal leaching after several reuses³¹. BET measurement provided evidence of the mesoporous character of Al-SBA-15 with a surface area of 646 $\text{m}^2 \text{g}^{-1}$ and a pore diameter of 7.8 nm. These values were not significantly reduced upon Au incorporation (see SI). XRD diffractograms revealed the presence of gold on the Al-SBA15 (see SI), with a calculated average nanoparticle size of ca. 25-30 nm using the Scherrer equation. The presence of such large Au aggregates could only be visualized in certain TEM micrographs while most TEM images (Figure 1, see also SI for a number of TEM images of Au@Al-SBA-15) showed the presence of highly dispersed Au nanoparticles with particle sizes <5 nm. XPS measurements proved the existence of mostly Au(0) in the materials (>80% Au) as demonstrated by Au_{4f} peaks at 83.6 and 87.3 eV (Figure 2 and SI). The existence of some Au³⁺ species (bands at 85.7 and 89.4 eV) could also be observed in XPS results.

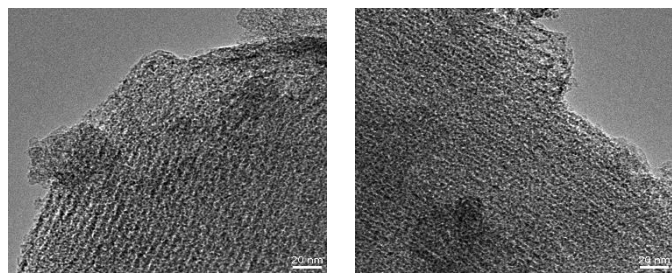


Figure 1: TEM images of Au@Al-SBA15 catalyst.

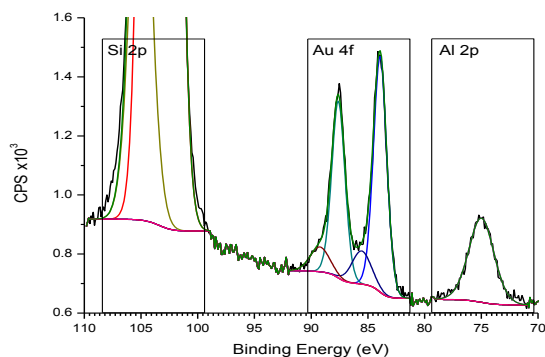


Figure 2: XPS measurements of Au@Al-SBA15 catalyst.

For the reaction optimization we chose a substrate bearing a sterically non-hindered terminal alkyne, which reacts much faster than an internal alkyne.^[15] The optimization of reaction conditions is reported on Table 1.

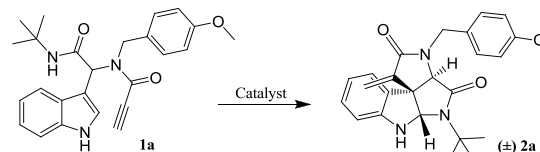


Table 1: Optimization of the reaction conditions.^[a]

entry	mol%	Solvent	Temp [°C]	t [h]	% Conv. ^[b] (% Yield) ^[f]
1 ^[b]	4.5	DCE	50	24	-
2 ^[b]	4.5	DCE	60	72	93 (92)
3 ^[b]	10	DCE	60	48	96
4 ^[b]	4.5	DCE	70	24	76
5 ^[b]	4.5	toluene	70	24	53
6 ^[b]	4.5	CHCl_3	70	24	60
7 ^[b]	4.5	ACN	70	24	88
8^[b]	10	DCE	70	3	100 (94)
9 ^[b]	10	toluene	70	3	74
10 ^[b]	10	CHCl_3	70	3	77
11 ^[b]	10	ACN	70	3	60
12^[b]	10	EtOH	70	3	100 (95)
13 ^[b]	10	H_2O	70	24	-
14 ^[b]	10	$\text{H}_2\text{O}/\text{EtOH}^{\text{[d]}}$	70	24	30
15 ^[c]	10	EtOH	70	3	91
16 ^[c]	4.5	EtOH	70	3	78
17 ^[h]	10	EtOH	70	3	10
18 ^[h]	10	EtOH	70	3	11
19 ^[h]	10	EtOH	70	3	11
20 ^[i]	10	EtOH	70	3	30
21 ^{[b],[g]}	10	EtOH	100	10min	100 (95)
22 ^{[c],[g]}	4.5	EtOH	100	10min	100 (95)
23 ^{[c],[g]}	2	EtOH	100	20min	100
24 ^{[c],[g]}	1	EtOH	100	30min	56
25 ^{[c],[g]}	0.5	EtOH	100	30min	32
26^{[c],[g]}	0.5	EtOH	110	20min	100 (96)
27	0	EtOH	110	60min	-

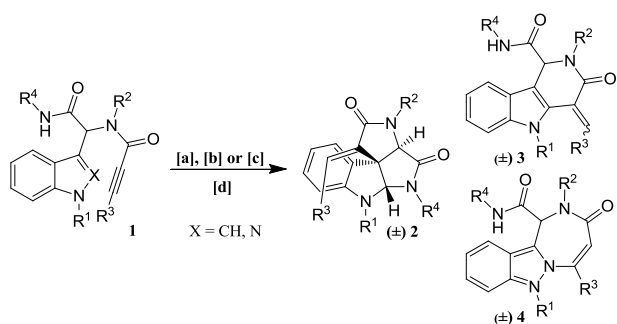
[a] All reactions were run with **1a** (12 μmol , 0.5 ml solvent) in a screw cap vial; [b] 4 wt% Au@Al-SBA15; [c] 2 wt% Au@Al-SBA15; [d] ratio of 1:1; [e] conversion determined by NMR-integration method; [f] isolated yields; [g] experiment was performed under μ -wave irradiation at a maximum power of 200 W; [h] 1 wt% Au on different types of reduced graphene; [i] 1 wt% Au@SBA15-APTES.

Gold nanoparticles supported on three different supports were selected, namely Al-SBA15, SBA15-APTES (a mesoporous silica modified with (3-aminopropyl)triethoxysilane) and various graphene materials with different quantities of Au. Reactions were conducted under conventional heating in both standard solvents typically used for gold catalysis as well as solvents with higher dielectric constants (entries 7, 11). Among the tested solvents, both ACN and EtOH worked well (entries 7, 11 and 12 respectively). Interestingly, in entry 14, the reaction proceeded to a limited extent in EtOH/water. Furthermore, reducing the mol% of gold in entry 16 resulted in a lower conversion rate, thus entry 12 was chosen as providing optimal conditions. Graphene-based supports used in entries 17-19 as well as SBA15-APTES supports used in entry 20 did not improve reaction yields under the investigated conditions. To improve reaction time, microwave heating was applied in entries 21-27. Satisfyingly, a temperature of 100 °C for 10 min resulted in 100 % conversion of **1a** in entry 21. In addition, we reduced the supported metal loading to 2 wt% in entries 22-26, without decreasing activity. The overall amount of metal was reduced to 0.5 mol% in entries 25-26. As proof of concept, a blank test with a metal free support was performed giving the predicted negative result in entry 27.

Using conventional heating conditions, we first investigated catalyst reusability through 12 consecutive runs (Table 1, entry 12). Reusability tests indicated the absence of Au leaching as measured by ICP-OES under the investigated conditions.³¹ Prior to the

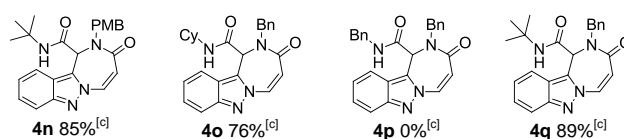
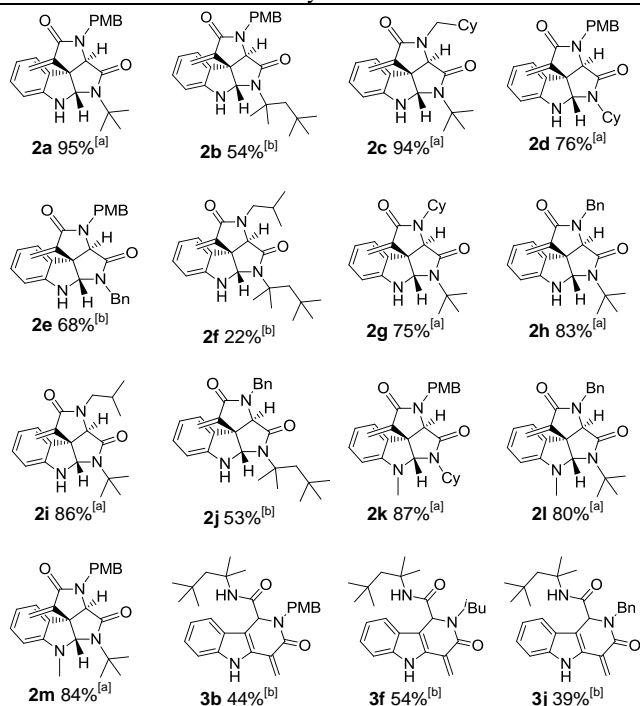
catalytic process in successive tests, the catalyst was separated by centrifugation and washed with EtOH until no more product was detected by TLC. After 12 cycles, the substrate was still converted 100 % selectively. The catalyst was then introduced in a study to determine the turn over number (TON). In this study, 2 mg of catalyst were introduced in a reaction with 220 mg of substrate. After stirring for 12 days at 70 °C the mixture was filtered and purified by column chromatography. We found a full conversion to product in the reaction which provided a minimum TON of 2599 (see SI).

The substrate scope for the reaction on terminal alkynes, as shown in Scheme 3, employing optimized conditions (Table 1, entry 26) was subsequently investigated and summarized in Chart 1. Good to excellent yields were achieved with exceptions for substrates **1b,f,j**. For those compounds not only was the formation of **2** observed, but a product with higher polarity was also detected by TLC monitoring. ¹H-NMR spectroscopy revealed the expected rearranged product containing the six-membered ring and free amide (**3b,f,j**; see SI for mechanism). This is most probably attributed to the steric hindrance exerted by the bulky R⁴-substituent, hampering trapping of the iminium moiety by the amide in the spiro-intermediate.^[7]



Scheme 3: Gold catalyzed post-Ugi cyclization giving three different products.

Chart 1: Results for terminal alkynes.



[a] 0.5 mol% Au as 2 wt% Au@Al-SBA15, EtOH, 110 °C, 20 min, MW (max. 200 W); [b] 0.5 mol% as 2 wt% Au@Al-SBA15, EtOH, 110 °C, 60 min, MW (max. 200 W); [c] 1.0 mol% as 2 wt% Au@Al-SBA15, EtOH, 110 °C, 60 min, MW (max. 200 W); [d] all reactions were run with 60 μmol of substrate in 1 mL of solvent.

Compounds **1n-q** bearing an indazole moiety resulted in different products, undergoing an endo-dig cyclization process. In this case exclusive formation of a novel diazepino[1,2-*b*]indazole skeleton was observed, as was proven by X-Ray crystal structure analysis of **4n** (see SI). The optimization for substrates bearing non-terminal alkynes is presented in Table 3. Here we started by using reaction conditions from Table 1 in entry 22. Unfortunately less than 10 % conversion was achieved (Table 3, entry 1). However, referring to the communication by Stratakis¹⁵ *et al.*, this was predictable due to the sterically hindering substituent on the triple bond. Therefore, the temperature was raised to 120 °C and the reaction was performed for 1.5 h under microwave heating as in Table 3, entry 3. Unfortunately these conditions resulted in substantial degradation giving several unidentified products. Thus we decided to apply conventional heating conditions similar to those mentioned in Table 1, entry 12, but at a slightly elevated temperature of 80 °C for 48 h. Satisfyingly the reaction proceeded with full conversion and **2r** was isolated with an excellent yield of 94 % (entry 5).

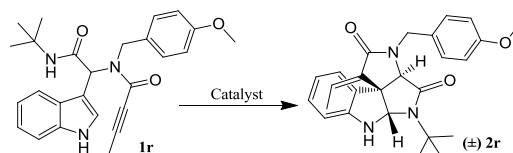
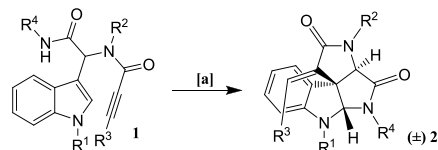


Table 3: Optimization of the reaction conditions.

entry ^[a]	mol% Au	Solvent	Temp [°C]	t [h]	% Conv. ^[d] (% Yield) ^[e]
1	4.5	EtOH	100	10min	< 10
2	4.5	EtOH	100	2	< 10
3	4.5	EtOH	120	1.5	90 (degr.)
4 ^[b]	10	EtOH	100	3	< 10
5 ^{[b],[c]}	10	EtOH	80	48	100 (94)
6	10	DCE	110	3	100 (degr.)

[a] All reactions were performed with 12 μmol of **1r** under microwave irradiation at a maximum power of 200 W in 1 mL of solvent; the catalyst contained 2 wt% Au@Al-SBA15, [b] 4 wt% Au@Al-SBA15 was used as the catalyst; [c] the reaction was performed under conventional heating; [d] conversion determined by NMR; [e] isolated yields.

The scope of the protocol was subsequently investigated and is shown in Chart 2. Not entirely unexpectedly we noticed that, the larger the alkyne substituent is, the worse the reaction performs. Changing the substituent from a methyl-group to an ethyl-group resulted in a drop of yield by 76 % (**2r**, **2t**).

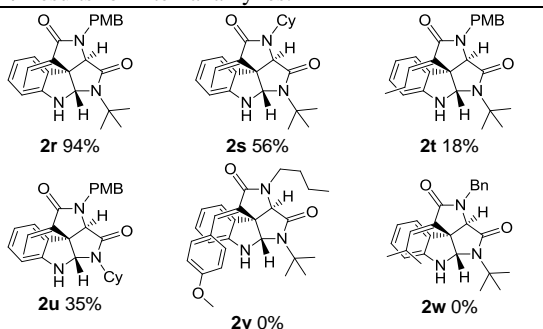


Scheme 5: Gold catalyzed post-Ugi cyclization of internal alkynes.

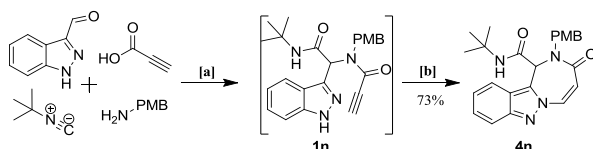
We finally investigated the possibility to perform the sequence as a one-pot cascade reaction, starting from indazole-3-carbaldehyde, which can be seen in Scheme 6. All components for the Ugi reaction as well as the catalyst for the cyclization were pre-mixed. To our

delight the reaction proceeded well, delivering compound **4n** in 73 % yield. The formation of **4n** does not work employing homogeneous conditions, probably due to an unyielding coordination of the isonitrile to the cationic gold complex. Unfortunately when switching to indole-3-carbaldehyde, no Ugi-product was formed.

Chart 2: Results for internal alkynes.



[a] 10 mol% Au as 4 wt% Au@Al-SBA15, EtOH, 80 °C, 48 h, conventional heating, 60 μmol of substrate in 1 mL of solvent.



Scheme 6: One-pot cascade reaction. [a] 60 μmol of propiolic acid, tert-butyl isonitrile (1.0 equiv), para-methoxybenzylamine (1 equiv), 1H-indazole-3-carbaldehyde (1.1 equiv), MS 4Å, EtOH (2 mL), 50 °C, 22 h; [b] 2 mol% Au as 2 wt% Au@Al-SBA15, EtOH (2 mL), 110 °C, MW at a maximum power of 200 W, 60 min.

Conclusions

We developed an attractive and green approach to synthesizing complex spirocyclic structures with three to four points of diversity by employing supported gold nanoparticles. A one-pot cascade reaction was presented which exclusively leads to the desired diazepino[1,2-*b*]indazole **4n**. This one-pot reaction is not applicable when originating from indole-3-carbaldehyde. Further studies on the improvement of the process for substrates bearing internal alkynes and the role of gold nanoparticle size distribution are currently under investigation. The simple and reproducible preparation, handling and reusability properties of the proposed system feature mechanochemically synthesized nanomaterials as excellent tools for organic transformations.

Acknowledgements

FS is grateful to the Agency for Innovation by Science and Technology (IWT) for providing a PhD scholarship. We thank Geert Hooyberghs and Dipak D. Vachhani for valuable discussions and the Hercules Foundation for supporting the purchase of equipment through the project AKUL/09/0035, Molybdenum high-energy X-ray source for in-situ diffraction studies of advanced materials and single crystals.

Notes and references

^aUniversity of Leuven (KU Leuven), Department of Chemistry, Laboratory for Organic & Microwave-Assisted Chemistry, Celestijnenlaan 200F, B-3001, Leuven, Belgium

^bUniversidad de Córdoba, Departamento de Química Orgánica, Campus de Rabanales, Edificio C-3 (Marie Curie – Anexo), Carretera Nacional IV – A, Km. 396, 14014 Córdoba, Spain

^cTechnische Universiteit Eindhoven, Department of Chemical Engineering and Chemistry, Micro Flow Chemistry and Process Technology, Den Dolech 2, 5600 MB Eindhoven, Netherlands

^dGent University, Department of Organic and Macromolecular Chemistry, Laboratory for Organic and Bioorganic Synthesis, Krijgslaan 281, S4, B-9000, Gent, Belgium

Electronic Supplementary Information (ESI) available: General experimental procedures; XRD, BET, TEM Characterization & Discussion of the catalyst; ¹H-NMR, ¹³C-NMR spectra and HRMS results of starting materials and products; X-Ray crystal structure of **4n**. See DOI: 10.1039/c000000x/

1. L. Fensterbank and M. Malacria, *Acc. Chem. Res.* 2014, **47**, 953-965.
2. A. S. K. Hashmi, *Acc. Chem. Res.* 2014, **47**, 864-876.
3. C. Obradors and A. M. Echavarren, *Acc. Chem. Res.* 2014, **47**, 902-912.
4. Y.-M. Wang, A. D. Lackner and F. D. Toste, *Acc. Chem. Res.* 2014, **47**, 889-901.
5. D.-H. Zhang, X.-Y. Tang and M. Shi, *Acc. Chem. Res.* 2014, **47**, 913-924.
6. X. Moreau, J.-P. Goddard, M. Bernard, G. Lemière, J. M. López-Romero, E. Mainetti, N. Marion, V. Mourières, S. Thorimbert, L. Fensterbank and M. Malacria, *Adv. Synth. Catal.* 2008, **350**, 43-48.
7. S. G. Modha, A. Kumar, D. D. Vachhani, J. Jacobs, S. K. Sharma, V. S. Parmar, L. Van Meervelt and E. V. Van der Eycken, *Angew. Chem. Int. Ed.* 2012, **51**, 9572-9575.
8. E. Van der Eycken, S. Modha, A. Kumar, D. Vachhani, S. Sharma and V. Parmar, *Synthesis* 2013, **45**, 2571-2582.
9. A. Fürstner and P. W. Davies, *Angew. Chem. Int. Ed.* 2007, **46**, 3410-3449.
10. D. J. Gorin and F. D. Toste, *Nature* 2007, **446**, 395-403.
11. J. H. Teles, S. Brode and M. Chabanas, *Angew. Chem. Int. Ed.* 1998, **37**, 1415-1418.
12. A. Homs, I. Escofet and A. M. Echavarren, *Org. Lett.* 2013, **15**, 5782-5785.
13. F. Schröder, C. Tugny, E. Salanouve, H. Clavier, L. Giordano, D. Moraleda, Y. Gimbert, V. Mourières-Mansuy, J.-P. Goddard and L. Fensterbank, *Organometallics* 2014, **33**, 4051-4056.
14. D. Wang, R. Cai, S. Sharma, J. Jirak, S. K. Thummanapelli, N. G. Akhmedov, H. Zhang, X. Liu, J. L. Petersen and X. Shi, *J. Am. Chem. Soc.* 2012, **134**, 9012-9019.
15. C. Gryparis, C. Efe, C. Raptis, I. N. Lykakis and M. Stratakis, *Org. Lett.* 2012, **14**, 2956-2959.
16. M. García-Mota, N. Cabello, F. Maseras, A. M. Echavarren, J. Pérez-Ramírez and N. Lopez, *ChemPhysChem* 2008, **9**, 1624-1629.
17. A. Kumar, D. D. Vachhani, S. G. Modha, S. K. Sharma, V. S. Parmar and E. V. Van der Eycken, *Beilstein J. Org. Chem.* 2013, **9**, 2097-2102.
18. D. D'Amours, F. R. Sallmann, V. M. Dixit and G. G. Poirier, *J. Cell Sci.* 2001, **114**, 3771-3778.
19. P. Siengalewicz, T. Gaich and J. Mulzer, *Angew. Chem. Int. Ed.* 2008, **47**, 8170-8176.
20. C. Gonzalez-Arellano, A. Abad, A. Corma, H. Garcia, M. Iglesias and F. Sanchez, *Angew. Chem. Int. Ed.* 2007, **46**, 1536-1538.
21. D. Tang, Z. Chen, J. Zhang, Y. Tang and Z. Xu, *Organometallics* 2014, **33**, 6633-6642.
22. X. Liu, L. He, Y.-M. Liu and Y. Cao, *Acc. Chem. Res.* 2014, **47**, 793-804.
23. A. Corma and H. Garcia, *Chem. Soc. Rev.* 2008, **37**, 2096-2126.
24. J. M. Campelo, D. Luna, R. Luque, J. M. Marinas and A. A. Romero, *ChemSusChem* 2009, **2**, 18-45.
25. R. J. White, R. Luque, V. L. Budarin and J. H. Clark, *Chem. Soc. Rev.* 2009, **38**, 481-494.
26. M. Al-Naji, A. M. Balu, A. Roibu, M. Goepel, W.-D. Einicke, R. Luque and R. Glaser, *Catal. Sci. Technol.* 2015, 10.1039/C4CY01174K.
27. A. Mariana Balu, A. Pineda, K. Yoshida, J. Manuel Campelo, P. L. Gai, R. Luque and A. Angel Romero, *Chem. Commun.* 2010, **46**, 7825-7827.
28. A. M. Balu, A. Pineda, D. Obermayer, A. A. Romero, C. O. Kappe and R. Luque, *RSC Adv.* 2013, **3**, 16292-16295.
29. M. Ojeda, A. Pineda, A. A. Romero, V. Barrón and R. Luque, *ChemSusChem* 2014, **7**, 1876-1880.
30. M. Ojeda, A. M. Balu, V. Barron, A. Pineda, A. G. Coletto, A. A. Romero and R. Luque, *J. Mater. Chem. A*, 2014, **2**, 387-393.

31. Preliminary data on the leaching behaviour of the metal was obtained in a continuous flow setup, in which a fixed bed reactor filled with 2% Au@Al-SBA15 was utilized for the same type of reactions presented in this paper. At 120 °C EtOH flew through the reactor and 5 samples with each 1 ml were taken. After evaporation of the solvent the samples were analysed by ICP-OES. The gold content of the samples was under the detection limit of the ICP-OES, thus suggesting that any leaching must be under 90 ng/mL.